climate

MDPI

*Article*

# Assessing Potential Links between Climate Variability and Sea Levels along the Coasts of North America

**Jason Giovannettone [1,*], Franklin Paredes-Trejo [2], Venerando Eustáquio Amaro [3] and Carlos Antonio Costa dos Santos [4]**

[1] Sisters of Mercy of the Americas, Silver Spring, MD 20910, USA
[2] Department of Civil Engineering, University of the Western Plains Ezequiel Zamora, San Carlos Campus, Barinas 2201, CO, Venezuela
[3] Departamento de Engenharia Civil, Universidade Federal do Rio Grande do Norte, Campus Universitário Lagoa Nova, Lagoa Nova, Natal 59078-970, RN, Brazil
[4] Unidade Acadêmica de Ciências Atmosféricas, Universidade Federal de Campina Grande, Av. Aprígio Veloso, Campina Grande 58109-970, PB, Brazil
* Correspondence: jgiovannettone@sistersofmercy.org; Tel.: +1-6125546159

**Abstract:** In order to better understand the extent to which global climate variability is linked to long-term mean and extreme sea level patterns, correlations between average sea levels at coastal sites throughout North America and low-frequency oscillations of several climate indices (CIs) were analyzed for the entire period of 1948–2018 as well as three equal-length sub-periods using correlation analysis. Correlation strength was assessed using Pearson's correlation coefficient, while significance was estimated using Leave-One-Out Cross-Validation and a bootstrapping technique ($p$-value). The sliding window size, lag time, and beginning month were varied for optimal correlation; 60-month sliding windows, along with 0 lag time, resulted in the strongest correlations. Strong (r >= 0.60) and significant ($p$-value <= 0.05) correlations were identified. The Western Hemisphere Warm Pool Eastern Asia/Western Russia index and ENSO exhibited the strongest and most widespread correlation with coastal sea levels. Further analysis was performed to identify and quantify the magnitude of any sea level trends using the Theil–Sen estimator, while the Mann–Kendall (MK) test was used to estimate the significance of said trends. The results revealed that a complex set of ocean–atmosphere interactions govern long-term coastal sea level variability in large coastal regions of North America. The final results of this study allow a greater understanding of potential links between climate variability and long-term sea levels along the coasts of North America, as well as insights into sudden shifts in these relationships, which will contribute toward more accurate long-term forecasts.

**Keywords:** climate variability; climate indices; low-frequency oscillations; sea levels; MJO; ENSO



**Citation:** Giovannettone, J.; Paredes-Trejo, F.; Amaro, V.E.; Santos, C.A.C.d. Assessing Potential Links between Climate Variability and Sea Levels along the Coasts of North America. *Climate* **2023**, *11*, 80. https://doi.org/10.3390/cli11040080

Academic Editor: Nir Y. Krakauer

Received: 26 January 2023
Revised: 28 March 2023
Accepted: 30 March 2023
Published: 3 April 2023



## 1. Introduction

The increasingly intense and frequent effects of weather extremes due to climate change have enhanced interest in risk management, sustainability development, resilience, and climate adaptation, especially in coastal areas [1–4]. Sea level rise in particular is receiving increasing attention among researchers, international agencies, non-governmental organizations, and policymakers due to the negative implications for coastal ecosystems and infrastructures [5]. Reguero et al. [3] argue that population growth and economic development within coastal zones coincide with increasing extreme sea levels associated with more frequent and intense coastal storms and, consequently, coastal vulnerability to disasters [6,7]. The global population living in portions of the coastal zone at elevations below 20 m is expected to rise by up to 71% by 2050 compared to the year 2000 [8]. Within the Western Hemisphere specifically, several coastal cities in South America, Central America, and North America are considered hotspots due to their high vulnerability to sea level rise and the absence of urgent adaptation plans [9,10], especially as climate change is

projected to exacerbate any potential impacts due to sea level rise [11]. It is projected that a sea level rise of 0.9 m by 2100 will place 4.2 million people living within coastal counties in the United States (US) alone at risk of flooding, while a rise of 1.8 m will affect 13.1 million people [12]. An additional concern is the fact that sea level rise has recently experienced a substantial acceleration. Nagy et al. [13] surmised that global sea levels have risen at an average rate of 3.2 mm $yr^{-1}$ since 1993, which is almost double the average rate since 1900 (1.7 mm $yr^{-1}$) [14].

The rates of sea level rise are not consistent globally or even regionally. For example, Watson [15] observed average rates of 2.19 $\pm$ 0.58 mm/year and 1.20 $\pm$ 0.45 mm/year when comparing the US Atlantic Coast/Gulf of Mexico to the Pacific West Coast, respectively. Various factors have been linked to changes in sea levels, including thermal expansion, isostatic rebound due to glacial retreat, changes in ocean dynamics, and land ice loss due to climate change; there is very high confidence that the combination of glacier and ice sheet melt is currently the dominant source of sea level rise, much of which is due to anthropogenic forcing [16]. There is also high confidence that other non-climatic forcing such as anthropogenic subsidence due to increased settlement and infrastructure development along the coasts as well as groundwater extraction affects coastal vulnerability to changes in sea levels as well.

In addition to the various types of anthropogenic forcing summarized above, recent studies have also suggested that long-term changes in coastal sea levels (and thus coastal vulnerability to the impacts of sea level rise) can be partly attributed to links between changes in atmospheric conditions (e.g., atmospheric pressure, direction and intensity of trade winds, etc.), as characterized by the El Niño/Southern Oscillation (ENSO), Pacific Decadal Oscillation (PDO), and North Atlantic Oscillation (NAO), as well as ocean heat content and sea surface temperatures (SSTs), as characterized by such climate indices (CIs) as the Atlantic Multidecadal Oscillation (AMO) and the Western Hemisphere Warm Pool (WHWP).

ENSO represents the dominant mode of interannual coupled atmospheric–oceanic variability [17] and is defined by shifting differences in atmospheric pressure between Tahiti and Darwin, Australia. El Niño (La Niña) is associated with higher (lower) pressure in Darwin and lower (higher) pressure in Tahiti, resulting in a decrease (increase) in the magnitude of the easterly trade winds. Lower (higher) magnitude easterlies result in less (more) water being transported toward the western Pacific, resulting in higher (lower) than normal sea levels throughout the eastern Pacific (along with warmer SSTs), including the west coasts of South, Central, and North America [18]. As a result, El Niño has not only been linked to higher sea levels but also to increased high-tide flooding along the US West Coast [19] as well as storm surges and more extreme seasonal sea level changes [20]. Specific regions within the tropical Pacific from which SST anomalies are used to characterize the current phase of ENSO (along with other CIs that characterize regional SST anomalies) are illustrated in Figure 1a.

The PDO, like ENSO, is also characterized by two phases that are associated with atmospheric pressure and SST fluctuations, though on longer time scales. The positive phase is defined by below-average sea level pressures and anomalously cool SSTs in the North Pacific (refer to Figure 1b for approximate location) and warmer SSTs along the Pacific Coast; the reverse conditions define the negative phase. Lower pressures within the interior North Pacific during a positive phase results in a wind stress regime that suppresses sea level rise along the US West Coast [21] with a negative phase having the opposite effect. When considered in combination with the effects of ENSO, even stronger links with sea level are evident [22].

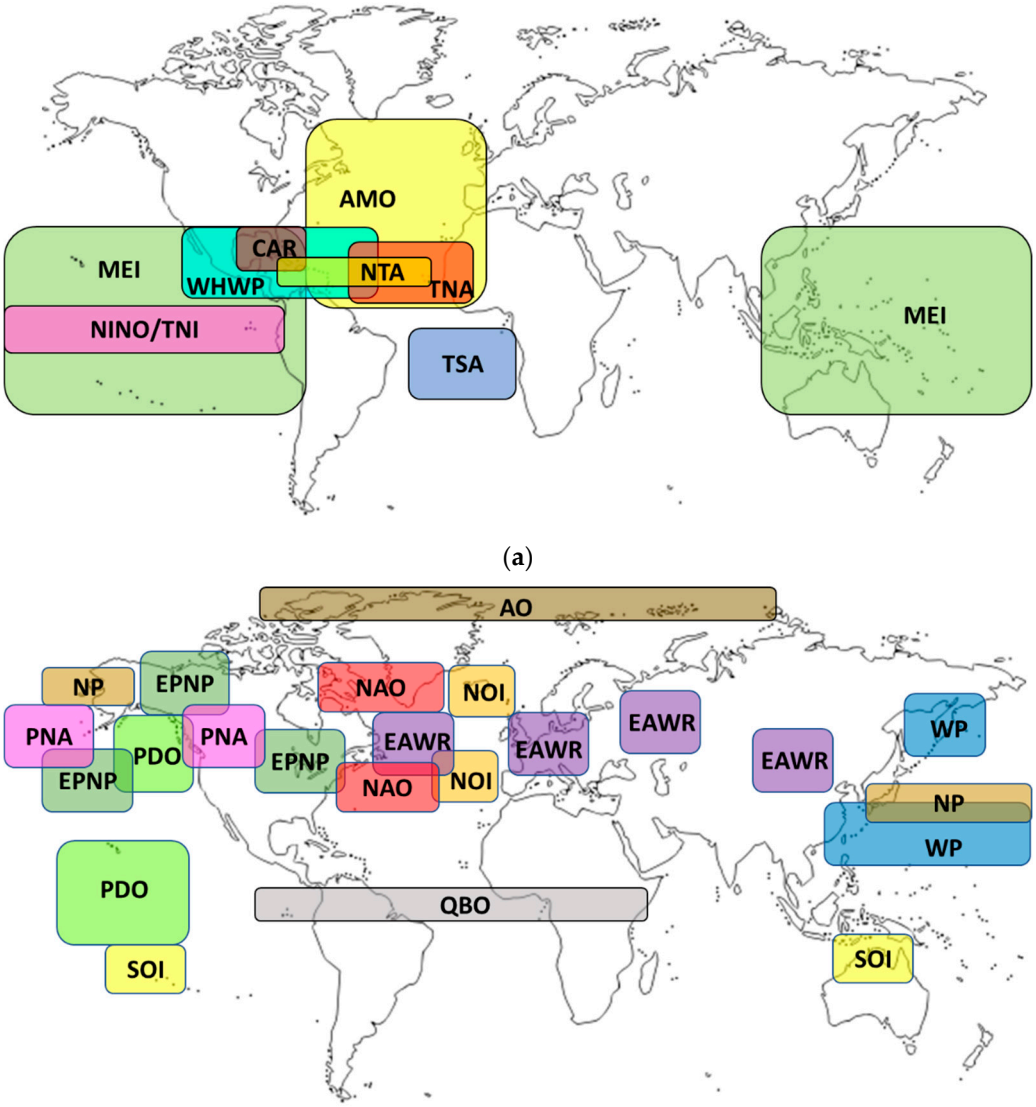


**Figure 1.** Locations characterized by various climate indices in terms of (**a**) SSTs and (**b**) atmospheric behavior (i.e., pressure and height anomalies). The CIs indicated by each abbreviation are defined in Table 1.

The situation along the US East Coast is a bit more complex. One of the key factors affecting East Coast sea levels is the strength of the Atlantic Meridional Overturning Circulation (AMOC), which is part of the global ocean current system transporting warm waters to the North Atlantic (see Buckley and Marshall [23] for a review of the AMOC). Much evidence has been found through numerical simulations and observational analyses for an inverse relationship between the meridional transport volume of water to the North Atlantic by the AMOC, which is indicative of the strength of the AMOC, and average coastal sea levels along the East Coast, although explaining smaller-scale variations along the coast has been more challenging [25]. As such, it can be surmised that any mechanisms of climate variability affecting the AMOC will impact coastal sea levels to an extent. For example, interannual variability in the AMOC (specifically during the winter months) has been linked to different phases of ENSO [26]. The AMOC was found to significantly weaken (strengthen) south (north) of 40 N during El Niño due to anomalously eastward (westward) wind stress that leads to anomalously positive (negative) turbulent heat flux into (from) the ocean in these areas. Opposite but slightly weaker effects were observed

during La Niña. As a result of this link between ENSO and the AMOC, a number of other studies have also identified a measurable link between sea levels along the East, as well as Gulf, Coasts and ENSO activity [27–31].

**Table 1.** CIs (abbreviations and names) assessed along with their respective periods of record. Detailed definitions of each climate index can be found at NOAA [24].

| CI (Abb.) | Climate Index | Beginning Year | Ending Year |
|---|---|---|---|
| AO | Arctic Oscillation | 1950 | 2018 |
| AMO | Atlantic Multidecadal Oscillation | 1948 | 2018 |
| CAR | Caribbean Index | 1950 | 2018 |
| EAWR | Eastern Asia/Western Russia | 1950 | 2013 |
| EPNP | East Pacific/North Pacific Oscillation | 1950 | 2018 |
| MEI | Multivariate ENSO Index | 1950 | 2018 |
| N12 | Niño 1 + 2 | 1950 | 2018 |
| N3 | Niño 3 | 1950 | 2018 |
| N34 | Niño 3.4 | 1950 | 2018 |
| N4 | Niño 4 | 1950 | 2018 |
| NAO | North Atlantic Oscillation | 1950 | 2018 |
| NP | North Pacific pattern | 1948 | 2018 |
| NTA | North Tropical Atlantic index | 1950 | 2018 |
| NOI | Northern Oscillation Index | 1948 | 2018 |
| PDO | Pacific Decadal Oscillation | 1948 | 2018 |
| PNA | Pacific North American index | 1950 | 2018 |
| QBO | Quasi-Biennial Oscillation | 1948 | 2018 |
| SOI | Southern Oscillation Index | 1951 | 2018 |
| TNI | Trans-Niño Index | 1948 | 2018 |
| TNA | Tropical Northern Atlantic index | 1948 | 2018 |
| TSA | Tropical Southern Atlantic index | 1948 | 2018 |
| WHWP | Western Hemisphere Warm Pool | 1948 | 2018 |
| WP | Western Pacific index | 1950 | 2018 |

Interannual sea level variability at locations along the US East Coast, particularly north of Cape Hatteras, has not only been found to be linked to the strength of the AMOC but also to storm surge activity associated with the frequency of tropical cyclones as well as local wind stress. Local winds can be influenced by any type of cyclical pressure pattern, the most dominant of which (on an interannual time scale) over the northern Atlantic Ocean is the NAO [32]. The positive phase of the NAO is associated with a stronger pressure gradient between the Icelandic low and the Azores high (see Figure 1b). As the pressure gradient strengthens, storm surge and tropical cyclone activity are enhanced along the northern East Coast [33] due to the creation of an expanded area exhibiting prime growth conditions that are closely aligned with the primary storm tracks. Local wind stress due to shifts in the NAO has also been found to influence regional sea levels along the northern East Coast, albeit this link has been found to be inconsistent throughout the last several decades [34].

In addition to the NAO and other climate indices that characterize atmospheric conditions over the North Atlantic (e.g., Arctic Oscillation (AO), Eastern Atlantic Western Russia pattern (EAWR), Northern Oscillation Index (NOI); refer to Figure 1b), there are various CIs that directly characterize SSTs throughout the North Atlantic as well (refer to Figure 1a), and therefore may represent a direct link with the strength of the AMOC and sea levels along the East Coast. The Atlantic Multidecadal Oscillation (AMO), for example, represents weighted mean SSTs over much of the North Atlantic (i.e., ~ 0 to 70 N) and, as such, has been closely linked to sea levels along the US coast through its influence on the AMOC [35] as well as on storm surge activity.

Further south, sea level rise south of Cape Hatteras, which has resulted in a higher frequency of nuisance flooding events along the coast, has been closely linked to the thermal expansion of ocean water due to a warming Florida Current [36]. The Florida Current

transports water from the Caribbean around the southern tip of Florida into the western Atlantic where it becomes the Gulf Stream. SSTs within the Western Hemisphere Warm Pool (WHWP), which represents an area of water warmer than 28.5 °C extending from the eastern North Pacific to the Gulf of Mexico and the Caribbean [37] and, as such, encompasses the entire Florida Current, has been closely linked to the temperature fluctuations of the Florida Current and recent sea level rise acceleration affecting southern portions of the East Coast [38]. As yet another mechanism by which ENSO affects East Coast sea levels is the fact that a warmer tropical North Atlantic caused by the weakening of the northeasterly trade winds during a Pacific Ocean El Niño event has been connected to warmer WHWP and Gulf of Mexico conditions through a "tropospheric bridge" [39]. Volkov et al. [40] also showed that atmospheric conditions associated with the NAO can foster large-scale heat divergence throughout the North Atlantic, thus affecting the temperature of the Florida Current and as well as sea levels along the East Coast.

In addition to detecting the presence of interannual and low-frequency climate signals linked to sea level variability, there is also a desire to identify any long-term trends that may exist in the sea level records. The multitude of CIs linked to sea level variability as well as the heterogeneous spatial distribution of tide gauges make the detection of long-term trends in relatively short sea level records [41] challenging. Thus, it is essential to use an appropriate technique to estimate sea level trends. One strategy is to fit a robust, linear regression model such as the Theil–Sen estimator to the data [42], while the Mann–Kendall (MK) test can be used to quantify the significance of the trend slope [43–45]. These methods are nonparametric and make no assumptions about the distribution of data. However, the MK test has limitations on autocorrelated time series. The trend significance is overestimated by positive autocorrelation and underestimated by negative autocorrelation in the time series. Consequently, the autocorrelation should be carefully considered to estimate the sea level trend within the time series from tide gauges through the MK test [46].

Several studies using the above-mentioned dual approach have revealed that changes in coastal seal level patterns are already evident in some coastal regions of the world. Aksoy [47] assessed the effects of the NAO on annual mean sea level data in the Black Sea and the Eastern Mediterranean Sea using MK z statistics. The results identified negative correlations for the Black Sea, whereas positive correlations were found for the Eastern Mediterranean Sea. Following a similar procedure, Taibi and Haddad [48] detected significant trends at 17 high-quality tide gauge stations along the Mediterranean Sea coast. On the US coast, Joshi et al. [46] investigated the changes in sea level at 95 tide gauge stations from the US National Oceanographic and Atmospheric Administration (NOAA) using MK and Pettitt's tests to estimate gradual trends and abrupt shifts, respectively. The authors found that most stations exhibited a positive sea level trend even after accounting for autocorrelation in the sea level records, suggesting that the trends and shifts were significant at most stations.

Based on the discussion above, the present study consists of two parts. First, due to the fact that much of the literature cited above focused on a small subset of climate indices ([49] being one exception) when attempting to identify links between extreme sea levels and climate variability, the current study considers, in addition to ENSO, a comprehensive set of CIs that includes those characterizing atmospheric activity (i.e., pressure and height anomalies) and SSTs over and within portions of the central and northern Pacific and Atlantic Oceans and the Caribbean. CIs include those discussed in addition to others (e.g., AO, East Pacific North Pacific index (EPNP), EAWR, NOI, North Pacific pattern (NP), West Pacific pattern (WP), etc.) for which it is plausible that similar links to sea levels exist. Refer to Figure 1 for the approximate locations of activity or SSTs characterized by each CI. Such an analysis identifies the potential spatial distribution of potential links between sea levels along the North American coasts and each CIs and contributes to a better characterization of both short-term and long-term future risk of coastal populations to the effects of climate variability on sea levels. The Theil–Sen estimator and the MK test are then used in an attempt to fit linear regression models to site data in order to identify

any significant trends and/or abrupt shifts in regional sea levels that have taken place. Section 2 discusses the data and methodology used to perform these assessments. The results are shown in Section 3, while a discussion of how the various CIs identified fit into the narrative formed by previous literature (discussed in the Introduction) is reserved for Section 4. Final conclusions are proposed in Section 5.

## 2. Materials and Methods

### *2.1. Data*

Monthly time series of mean sea level (ranging from 1948 to 2018) from the PSMSL (Permanent Service for Mean Sea Level) [50] tide gauge database were used. The reason behind the choice of this dataset is related to the fact that the PSMSL is one of the oldest long-term sea level information data services [51], and it has been extensively used in the Intergovernmental Panel on Climate Change assessment reports [52] and recent studies [9,42,47]. Therefore, the PSMSL dataset is considered a reliable dataset to assess potential links between coastal sea levels and various metrics of climate variability as well as any changes and trends in historic coastal sea levels. It is worth noting that monthly sea level time series can contain crucial information about the underlying physical processes that drive sea level variations. These processes include seasonal temperature changes and the El Niño–Southern Oscillation (ENSO) phases. However, these time series were not expressed as monthly anomalies to ensure that the underlying physical processes remain transparent in the applied analysis. This approach provides a more robust understanding of the dynamics driving sea level changes. More details on the PSMSL dataset are provided by Holgate et al. [51]. The study area and site locations (Figure 2) from which sea level data were collected encompass the coastal zones of North America and Mexico.

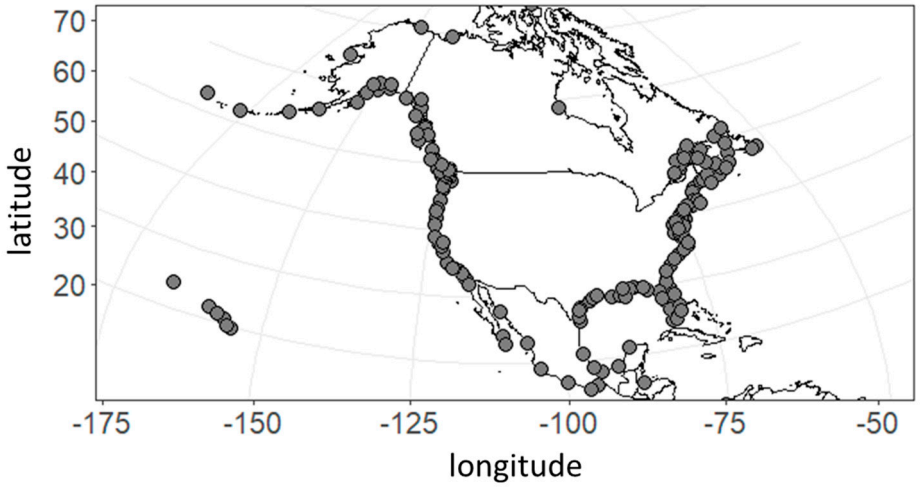


**Figure 2.** Locations of Permanent Service for Mean Sea Level (PSMSL) [49] sea level stations used throughout North America and Mexico.

Monthly mean CI data were obtained from the NOAA Physical Sciences Laboratory (PSL) [24]. The current study assessed several CIs (see Table 1 for CI names and periods of record) used to characterize SSTs and/or atmospheric pressure or height anomalies in the Atlantic and Pacific Oceans as well as the Caribbean. Only CIs for which links with coastal US sea levels have already been identified or that characterize activity or SSTs in areas similar to those already identified were considered. All CIs also have similar periods of record so as to ensure consistency in the final results. The interaction between changes in geology, dynamic ocean topography, and seafloor elevation is complex, which can make the attribution of coastal sea level changes to specific processes challenging. In light of these challenges, we opted to exclude these factors from consideration in this study.

### 2.2. Method

The study involved three steps in sequence. The first step was to collect the available coastal sea level data from the PSMSL database at locations along the coasts of North America and Mexico (Figure 2). A preliminary time window was defined from January 1948 to December 2018, in which the PSMSL database showed the lowest proportion of missing data for the study area [50]. To carry out the correlation and trend analyses in the following steps and determine if the results are consistent throughout the entire period of record, the study period was divided into three quasi-balanced epochs: 1948–1970 (23 years), 1971–1994 (24 years), and 1995–2018 (24 years). The epochal analysis was utilized to effectively capture the complex influence of various climatic factors, such as ocean currents, atmospheric pressure, and winds. This method is well-suited to studying the long-term trends and changes in sea level and their relationship to different climatic processes. Only those tide gauges whose sea level time series exhibited less than 10% of missing data during each time period were used in the analysis for that time period. Attempts were not made to fill in data gaps for those sites having greater than 10% of missing data for a particular time period; such sites were omitted from that time period's analysis. As a result, the number of sites analyzed in each of the three epochs was 43, 51, and 95, respectively.

The second step was to assess the correlation strength (Pearson's r statistic) and significance ($p$-value) between long-term mean sea levels at each site analyzed and the set of CIs listed in Table 1. The methodological scheme used by Giovannettone and Zhang [53] and Giovannettone et al. [54] for similar correlation analyses involving precipitation in North and South America was applied. This approach is based on a three-stage procedure. First, the correlation strength of sea levels (SL) with each CI was estimated using sliding windows defined by a range of sizes (W = 1–90 months), lag times (LT = 1–60 months), and beginning months (BM = 1 (i.e., January)–12 (i.e., December)). For each window size and beginning month, the mean sea level was computed using Equation (1):

$$\mathbf{SL_t} = \frac{1}{\mathbf{W}} \sum_{\mathbf{BM}}^{\mathbf{BM+W-1}} \mathbf{SL_m}, \quad (1)$$

where $\mathbf{SL_t}$ is the mean sea level for the sliding window beginning at month (m) = BM of year $t$ and ending at m = BM + W − 1. The mean climate indices were computed in a similar manner according to Equation (2):

$$\mathbf{CI_t} = \frac{1}{\mathbf{W}} \sum_{\mathbf{BM-LT}}^{\mathbf{BM-LT+W-1}} \mathbf{CI_m} \quad (2)$$

with the exception that the sliding window used for averaging is set back a number of months equal to LT. Similar to Giovannettone [55], only sites having a minimum of eight valid pairs of long-term mean SL/CI that contained zero missing values were considered. Second, the overall optimal window size and lag time were identified and then applied to all sites analyzed to ensure a consistent comparison between sites, while the optimal beginning window was varied between sites, leading to the identification of the dominant CI at each site in terms of the magnitude of linear correlation. Third, in order to account for the effects of spurious and serial correlation, cross-validation was initially performed following each correlation analysis using the Leave-One-Out Cross-Validation (LOOCV) technique [56], after which the statistical significance or $p$-value of each correlation for all sites analyzed was estimated using a bootstrap technique [57,58]. At this point, a strong and significant correlation was defined according to two criteria: (i) linear correlation (i.e., Pearson's r) greater than 0.60 and (ii) a $p$-value less than 0.05, which represents a rejection of the null hypothesis of no correlation at the 95% confidence level. The computations included in Step 3 were performed using an R script developed for this study as well as the HydroMetriks Climate Tool (Hydro-CLIM) developed by Giovannettone [59].

The third step was to apply the Mann–Kendall (MK) trend test and the Theil–Sen estimator to the original time series data (in contrast to the smoothed data used in the correlation analysis) to identify significant changes in coastal sea level in terms of trajectory and magnitude. Since the MK trend test is highly influenced by serial autocorrelation [47] that could be present in the sea level time series, the modified MK (m-MK) test proposed by Yue and Wang [44] was implemented at a 95% confidence level. Positive and significant scores indicate a trend of sea level rise at the local scale, and negative and significant scores indicate a decrease in sea level at the local scale. In addition, the Theil–Sen estimator reflects the magnitude of the slope for those reference sites with a significant trend. Both procedures were implemented under R using the 'modifiedmk' and 'mblm' packages. To enhance clarity, we employed a trend categorization approach to effectively differentiate statistically significant trends (i.e., decreasing or increasing) from insignificant ones (i.e., stable). This method helps to provide a clearer and more concise picture of the long-term changes in sea level, which is critical for understanding the underlying mechanisms driving sea level variations and predicting future changes.

## 3. Results

### *3.1. Multidecadal Coupling between the Coastal Sea Level and Different CIs*

Due to the amount of data available during the 1995–2018 epoch compared to the earlier epochs, preliminary results from the correlation analysis performed for the most recent sub-period were used to identify the optimal size of the sliding windows used to compute long-term mean values of sea levels and CI activity as well as the optimal lag time between the two windows so that the maximum correlation was obtained. The optimal sliding window size and lag time were then applied to the other epochs to facilitate consistent comparisons between each period and assess the persistence of any signals related to climate variability that were identified. Considering the two CIs that exhibited by far the most spatial dominance for the 1995–2018 epoch, Figure 3 shows the results for all sliding window lengths (using a zero lag and the optimal beginning month) for all sites where the Western Hemisphere Warm Pool (WHWP) (Figure 3a) or the Eastern Asia Western Russia index (EAWR) (Figure 3b) were found to exhibit a dominant signal. It can be seen in Figure 3a that the correlation of sea levels with the WHWP increased quickly up to a local maximum at a sliding window size of approximately 60 months, after which the increase in correlation was negligible. Figure 3b reveals similar behavior concerning the EAWR. Based on these preliminary results, as well as for the sake of consistency, a sliding window size of 60 months was selected for all sites and epochs analyzed within the current study.

Lag times ranging from 0 to 60 months were then tested over the 1995–2018 epoch using the optimal window size of 60 months. Because the optimal sliding window size is large and only sliding windows containing zero missing values were considered, the total number of data points available for this and future correlation analyses were greatly reduced. Analysis of these data revealed that the correlation of sea levels with the two dominant CIs, WHWP and EAWR, did not vary significantly with lag time, albeit with a slight peak observed at a lag time of 0 months. Based on these results, and for the sake of consistency, a lag time of 0 months and a sliding window size of 60 months were selected for all future correlation analyses.

Using the optimal sliding window properties identified above, the dominant CIs were identified for all sea level sites at which there were sufficient data (at least eight pairs) to do so during each epoch as well as over the entire period of record. As such, the numbers of sites considered for the full period of record analysis (1948–2018) and the 1948–1970, 1971–1994, and 1995–2018 epochs were 143, 43, 51, and 95, respectively. Of these sites, only those for which the dominant correlation was found to be both strong ($|r| >= 0.60$) and significant ($p$-value <= 0.05) were considered, which resulted in 96 sites (67%), 19 sites (44%), 22 sites (43%), and 69 sites (73%) being retained for each analysis, respectively.

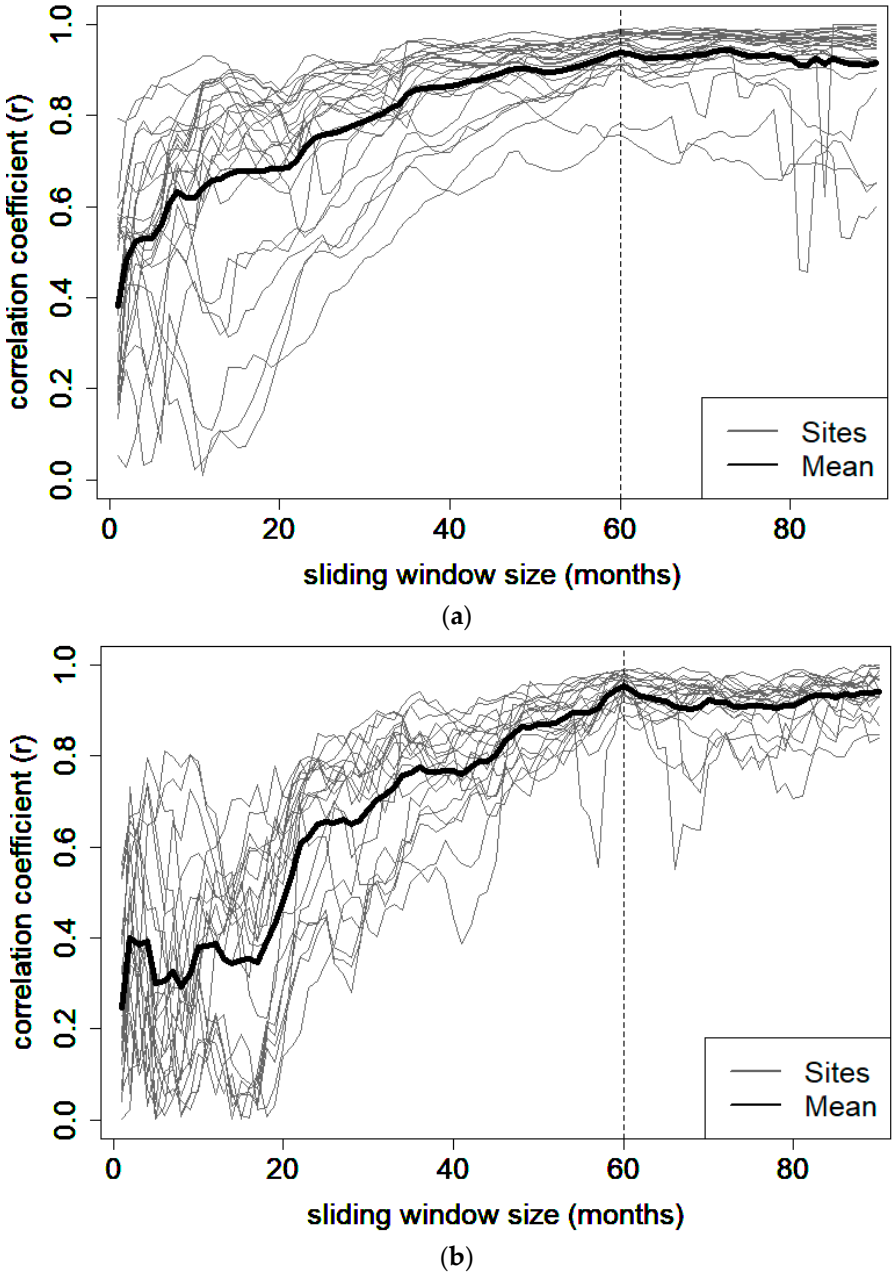


**Figure 3.** Resulting correlation magnitudes at sites along the coasts of North America (including the Great Lakes, Alaska, Hawaii, Puerto Rico, and Bermuda) and Mexico at which mean sea level correlates strongest with the (**a**) WHWP and (**b**) the EAWR using sliding windows sizes ranging from 1 to 90 months and lag time = 0 months over the time period of 1995–2018. The dotted lines indicate the selected optimal window size.

Figure 4 reveals the dominant CIs that were identified for each of the 96 sites using sea level and CI data taken from the entire period of record and using the criteria listed above; approximate regions over which each CI is characterized are shown in Figure 1. It should be noted that even though multiple CIs may exhibit strong and significance correlation with sea levels at a site, only the dominant CIs are indicated. As a result, sites located in close proximity to each other may exhibit dominant correlations with different CIs. A list of the most spatially dominant CIs that includes the percentage of sites at which they were identified as dominant is also provided in the first two columns of Table 2. The WHWP, TSA, and ENSO (as characterized by the CIs N12, N3, and MEI), exhibited the strongest links overall with long-term sea levels at the highest percentage of sites (29%, 18%, and

14% of valid sites, respectfully). Sea levels at sites along the US East and Gulf Coasts were primarily linked to the WHWP, TSA, and EAWR, which is consistent with the earlier discussion concerning potential mechanisms in and over the northern and central Atlantic Ocean affecting East Coast sea levels. The WHWP and ENSO (namely characterized by N12 and N3) exhibited spatial dominance along the West Coast.

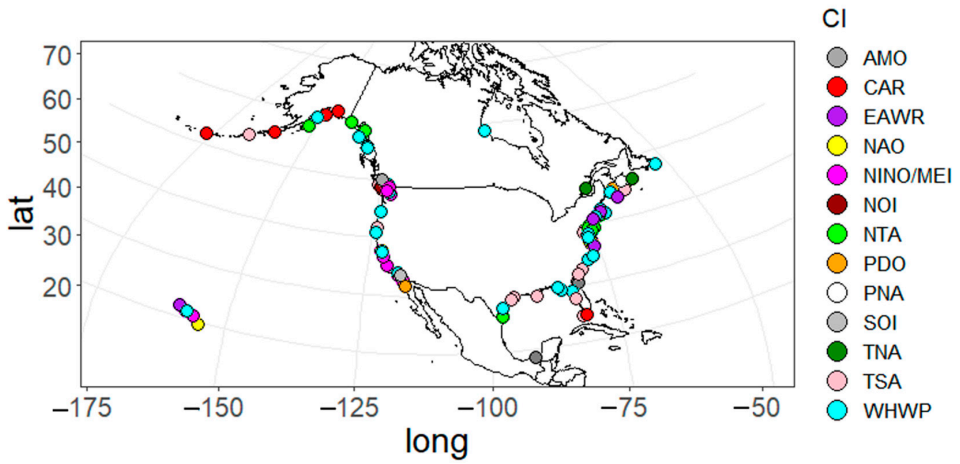


**Figure 4.** Illustration of CIs resulting in optimal correlation with mean sea level (window size = 60 months; lag = 0) for all sites at which |r| >= 0.60 and $p$ <= 0.05 throughout North America for the full period of record (1948–2018). (See Table 1 for CI abbreviations.).

**Table 2.** Lists of the dominant CIs that correlate with mean sea level and the percent of sites where |r| >= 0.60 and the $p$-value <= 0.05 using a sliding window size of 60 months and lag time = 0 over the following time periods: 1948–2018 (Columns 1 and 2), 1948–1970 (Columns 3 and 4), 1971–1994 (Columns 5 and 6), and 1995–2018 (Columns 7 and 8).

| CI | % Sites | CI | % Sites | CI | % Sites | CI | % Sites |
|---|---|---|---|---|---|---|---|
| WHWP | 29.2 | NINO/MEI | 26.3 | NINO/TNI | 40.9 | WHWP | 36.2 |
| TSA | 17.7 | AMO | 15.8 | NOI | 13.6 | EAWR | 29.0 |
| NINO/MEI | 14.5 | EAWR | 10.5 | TNA | 13.6 | NINO/TNI | 8.7 |
| NTA/TNA | 13.6 | CAR | 10.5 | WHWP | 9.1 | WP | 8.7 |
| EAWR | 6.3 | PDO | 10.5 | WP | 9.1 | CAR | 7.2 |
| CAR | 5.2 | NOI | 10.5 | EAWR | 4.5 | PDO | 2.9 |
| NAO | 4.2 | PNA | 5.3 | NAO | 4.5 | NAO | 1.4 |
| PDO | 3.1 | WHWP | 5.3 | SOI | 4.5 | NOI | 1.4 |
| PNA | 2.1 | WP | 5.3 | | | NP | 1.4 |
| AMO | 1.0 | | | | | NTA | 1.4 |
| NOI | 1.0 | | | | | SOI | 1.4 |
| NP | 1.0 | | | | | | |
| SOI | 1.0 | | | | | | |

In an attempt to determine if the links between sea levels and CIs identified in Figure 4 are consistent throughout the period of record (1948–2018), Figure 5 shows the dominant CI identified for each valid site using the criteria given above and epoch. It should again be noted that only the most dominant CIs are shown. A list of the dominant CIs as well as the percentage of sites at which they each found to be the most dominant are provided in Columns 3–8 of Table 2 for all epochs. Beginning with the first epoch (1948–1970), a substantially smaller number of sites containing sufficient valid data were available for further analysis. Of these sites, ENSO (as characterized by the CIs N12, N4, and MEI), the AMO, and the EAWR exhibited the strongest links with long-term sea levels at the highest percentage of sites (26%, 16%, and 11% of valid sites, respectfully), the locations of which are shown in Figure 5a. Although it was difficult to identify spatial coherence related to strong links between either CI and sea levels due to the limited data available spatially and temporally, sea levels at sites along the US East and Gulf Coasts were found to be primarily

linked to ENSO, AMO, and CAR, which is consistent with the earlier discussion concerning potential mechanisms affecting East Coast sea levels; strong signals related to the EAWR were also detected. Improved spatial coherence was observed for the 1971–1994 epoch with the EAWR dominating the strong linkages identified along the East Coast and ENSO, (namely characterized by N12, N34, and the Trans-Niño Index (TNI)) exhibiting spatial dominance along the West Coast (Figure 5b). These results are consistent with the results from Figure 4 as well as previous studies, although the dominance of the EAWR in both epochs over other Cis that characterize atmospheric conditions over the North Atlantic was unexpected and so far, undocumented.

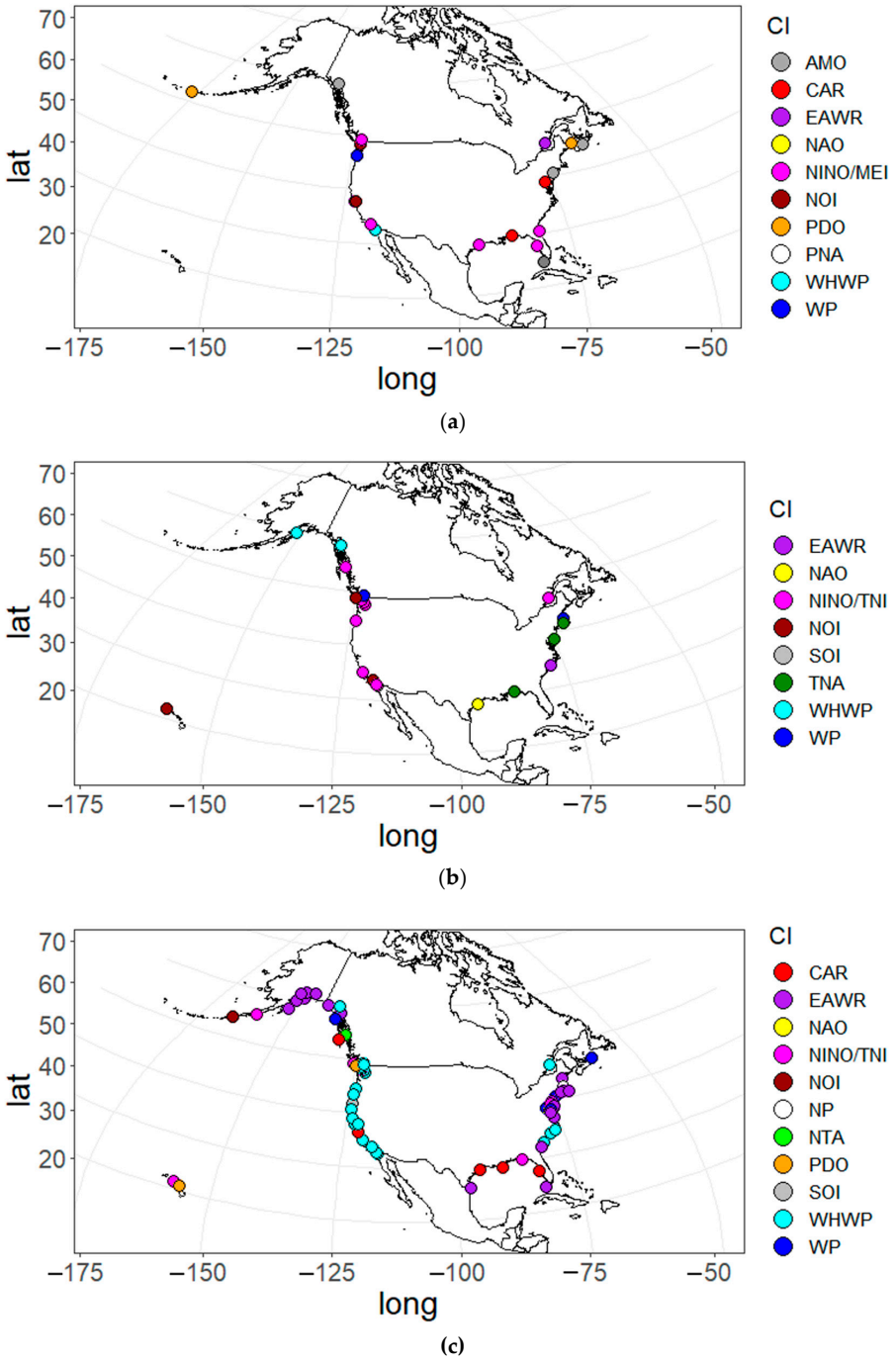


**Figure 5.** As in Figure 4, except for the epochs (**a**) 1948–1970, (**b**) 1971–1994, and (**c**) 1995–2018. (See Table 1 for CI abbreviations.).

In the most recent epoch (i.e., 1995–2018), the WHWP and the EAWR exhibited dominant and spatially coherent signals at a majority of valid sites (Table 2). In particular, the WHWP exhibited a strong signal with long-term sea level variability (mean $|r| = 0.918$) along the entire US West Coast as well as the portion of the East Coast south of Cape Hatteras, North Carolina (Figure 5c); this is consistent with the results from Figure 4 regarding the entire period of record. The EAWR also showed exceptionally strong signals (mean $|r| = 0.930$) in the northern Pacific along the coast of Alaska as well as along the US East Coast north of Cape Hatteras, which is in contrast to the other periods. The results concerning the coastal regions where strong links with the WHWP and EAWR were identified are in some respects consistent with previous studies mentioned earlier, particularly with regard to the significance of Cape Hatteras as a transition point between the coastal regions to the north where sea levels are most affected by atmospheric conditions over areas of the North Atlantic and regions to the south where sea levels are most affected by the strength and temperature of the Florida Current. Additional discussion is provided in Section 4. It is worth noting that some of the correlations identified in this study align with prior research in the scientific literature that also indicates potential modifications to sea level and tidal trends [60,61]. As such, it is important to evaluate whether there have been long-term trends at the level of the measuring stations and the sign of such trends in order to gain a more comprehensive understanding of what has occurred in each epoch. To this end, we will conduct a thorough analysis of this aspect in the following section. This will help us to enhance our understanding of the underlying physical processes that drive the observed coastal sea level changes.

### *3.2. Coastal Sea Level Trend for Each Epoch*

Figure 6 illustrates the sea level trends for distinct epochs, as determined by the modified Mann–Kendall test. Examining coastal sea level trends across three distinct epochs—1948–1970, 1971–1994, and 1995–2018—reveals significant variability in the northeastern US and Canadian coastal regions. In the 1948–1970 epoch, the coastal sea level increased in 24 reference sites in the northeastern US and Canada, excluding Florida. Among these, four sites exhibited a decline, while 14 remained stable. Approximately 28% of the sites exhibiting an increasing trend in coastal sea levels were predominantly influenced by the AMO, while the CAR and PDO each accounted for 20% of the sites. During the subsequent epoch, from 1971 to 1994, 26 out of 51 sites showed an increase in coastal sea level, 9 sites experienced a decrease, and 16 were stable. Roughly 19% of the sites exhibiting an increasing trend in coastal sea levels were primarily dominated by the WHWP, while the EAWR accounted for about 15% of the sites. Additionally, the N12 and NOI each contributed to less than 12% of the sites. In the final epoch, spanning 1995 to 2018, 59 sites registered an increase in coastal sea level, 13 sites experienced a decline, and 23 remained stable. Coastal sea levels increased in the eastern and western US, including Hawaii. In contrast, higher latitude sites in Canada showed opposite or stable signals. In approximately 43% of the sites displaying an increasing trend in coastal sea levels, the WHWP emerged as the dominant factor. The EAWR accounted for just under 21% of the sites, while the CAR contributed to slightly more than 10% of the sites.

Overall, coastal sea levels in the United States and Canada have undergone notable changes in the past 70 years (refer to Supplementary Tables S1–S3). Several sites, including Baltimore, Galveston II, Honolulu, San Diego, San Francisco, Seattle, and Solomon's Island, exhibited a persistent increase in coastal sea levels across all epochs under examination. Focusing on the final two epochs (i.e., 1971–2018), a marked increase in coastal sea levels was detected during this period at several additional US stations, including Key West, Lewes, Charleston I, Los Angeles, La Jolla, Annapolis, Newport, Friday Harbor, Port San Luis, St. Petersburg, Port Townsend, Beaufort, and Lewisetta. Conversely, coastal sea levels at Juneau, Sitka, and Seldovia were found to decrease throughout the final two epochs.

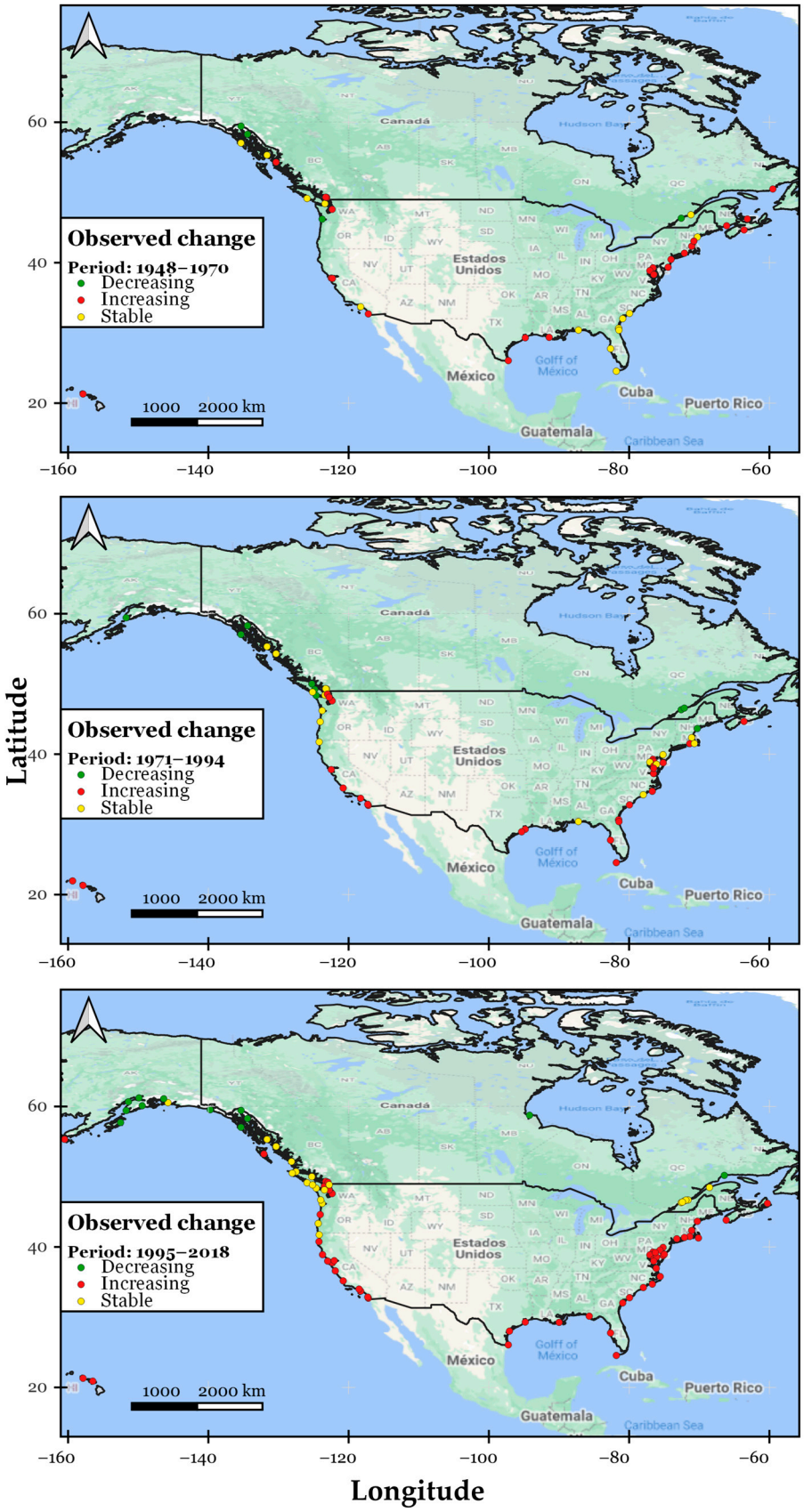


**Figure 6.** Spatial distribution of the trend in coastal sea levels using the modified MK test for the epochs: (**a**) 1948–1970, (**b**) 1971–1994, and (**c**) 1995–2018.

Figure 7 depicts the long-term coastal sea level trend at the San Francisco station. We used the LOcally WEighted Scatterplot Smoothing (LOWESS) method with a smoother span of 0.20 to increase clarity and reduce noise [62]. The results show an increasing trend across all three epochs. The mean coastal sea level rose from 7006.11 mm in Epoch 1 (1948–1970) to 7060.02 mm in Epoch 2 (1971–1994) and further to 7090.69 mm in Epoch 3 (1995–2018). Sea levels continued to rise throughout the study period, with an increase of 53.91 mm between Epochs 1 and 2 and an increase of 30.67 mm between Epochs 2 and 3. Notably, the dominant climate index changed in each epoch: EAWR in Epoch 1, NOI in Epoch 2, and WHWP in Epoch 3. Inter-annual variability was observed within each epoch, with fluctuations in coastal sea levels ranging from negative to positive anomalies. These variations are superimposed on a background of coastal sea level rise with significant future implications for coastal regions in San Francisco and may be partially attributed to natural climate variability.

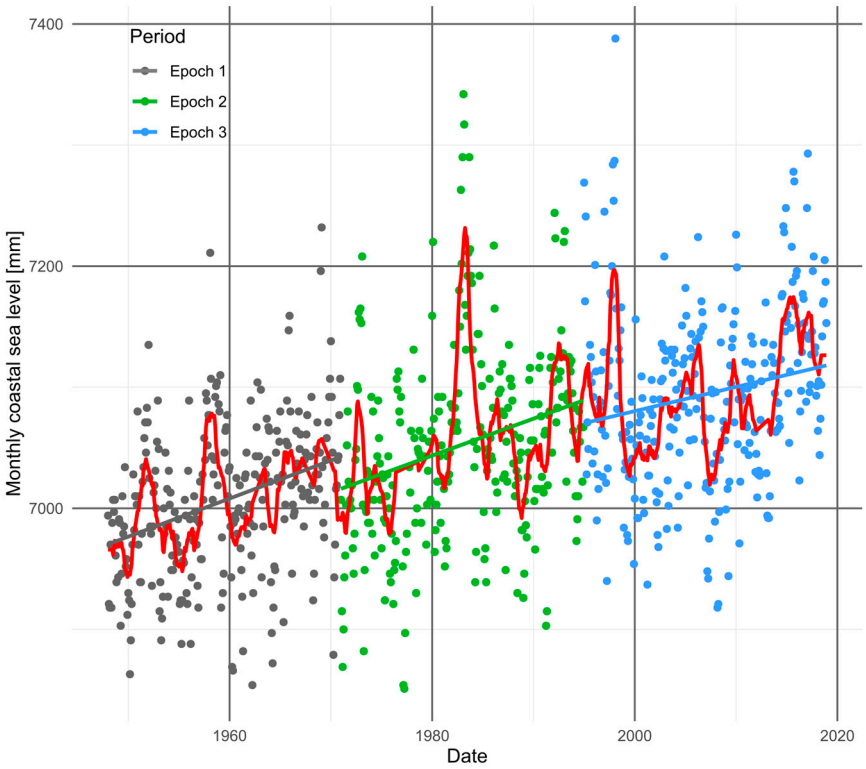


**Figure 7.** Coastal sea level trends at the San Francisco station for the periods 1948–1970 (grey), 1971–1994 (green), and 1995–2018 (blue). Observed records are represented by points, while the continuous red line depicts a smoothed output of the series using the LOWESS nonparametric regression approach.

## 4. Discussion

In this study, long-term coastal sea level trends and their potential relationships with various climate indices (CIs) were analyzed over the period of record from 1948 to 2018 as well as three equally divided epochs throughout this period to in an attempt to identify temporally and spatially consistent links between various mechanisms of climate variability and coastal sea levels at coastal sites along the coasts of North America and Mexico. Analysis of the full period of record revealed dominance by the WHWP along both the East and West Coasts, the TSA along the southern East and Gulf Coasts, and ENSO along the West Coast. These results are consistent with mechanisms identified in the literature as described above and, due to the higher data availability from using a longer period of record, serve as a basis by which to assess the reliability of the results shown for the shorter epochs.

Due to the fact that there were substantially fewer coastal sites containing sufficient valid data during the first two epochs (i.e., 1948–1970 and 1971–1994), it is difficult to identify any spatial patterns with confidence regarding the dominance of any particular CI. As already mentioned, the dominance of CIs characterizing ENSO, and the AMO and CAR, are consistent with previous studies mentioned earlier that have associated West and/or East Coast sea levels with SSTs in the Pacific and Atlantic Oceans as well as the Caribbean. The dominance of the EAWR is also consistent with studies that have associated atmospheric conditions (i.e., height and pressure anomalies) over the North Atlantic with East Coast sea levels, though it should be noted that the EAWR specifically has not been addressed with much of the focus being place on the NAO. The EAWR is of particular interest here as its link to East Coast sea levels to some extent persisted throughout all three epochs, though its apparent dominance is not obvious when considering the entire period of record.

Compared to the first two epochs, the final epoch (i.e., 1995–2018) exhibited substantially higher spatial coherence, particularly with regard to the dominance of the WHWP and EAWR on both the US and Canadian West Coasts and the US East and Gulf Coasts. As already discussed, the WHWP is known as the second-largest warm pool on the planet throughout the boreal summer [37], and, as such, has been found to act as a sort of trigger for ENSO events with anomalously low (high) SSTs within the WHWP seemingly initiating El Niño (La Niña) events with a 17-month lag [63] Therefore, an apparent strong correlation with the WHWP may represent a manifestation of the strong link between West Coast sea levels and ENSO that has already been identified as discussed earlier. Alternatively, the WHWP may have significant influence outside of its potential relationship with ENSO. The warm phase of the WHWP induces northerly wind anomalies over the North Pacific due to the westward propagation of Rossby waves at interannual and decadal time scales, which in turn, may disturb the migration of the Pacific Intertropical Convergence Zone [64]. This physical mechanism could favor the thermal expansion of the Pacific Ocean and indirectly increase coastal sea levels in the northeastern Pacific Ocean and along the US West Coast.

The dominant CIs identified during the final epoch along the US East Coast are consistent with the results of previous studies except for one difference. The current study identified a transition point at Cape Hatteras (North Carolina, USA at 35.24° N latitude and 75.52° W longitude), south of which the WHWP and the CAR were found to have strong links to long-term sea levels along the southern East Coast and Gulf Coast, respectively. Both CIs characterize SSTs throughout the Gulf of Mexico, though the WHWP covered a wider area that extends beyond the western coast of Mexico and east of the Caribbean (see Figure 1), while the CAR is focused only on the Caribbean. In any case, the dominant influence of both CIs is not surprising due to their close proximity to the Florida Current, and therefore would support the previous literature in terms of the effect of SSTs on the strength of the Florida Current and southern East Coast sea levels [38].

North of Cape Hatteras, the long-term sea levels were most closely linked to atmospheric activity over the North Atlantic (consistent with the findings of Pinto et al. [33] and Kenigson et al. [34]) and south of which sea levels were strongly linked to SSTs within regions that would significantly affect the Florida Current (consistent with the findings of Ezer et al. [36] and Domingues et al. [38]). North of Cape Hatteras, the EAWR represented the dominant CI along the entire mid-Atlantic and Northeast US coastline. As can be seen in Figure 1, the EAWR is represented by height anomalies located over four regions, including Europe, northern China, the central North Atlantic, and north of the Caspian Sea. The positive phase of the EAWR is characterized by positive (negative) anomalies over Europe and China (North Atlantic and north of the Caspian Sea), while reverse anomalies occur during the negative phase. As previous literature has identified the NAO as a major factor in sea level variability along the East Coast north of Cape Hatteras due to mechanisms discussed earlier, it is not surprising that dominant correlations with the EAWR were identified due to the fact that the North Atlantic height anomaly is located between the two regions of pressure anomalies that characterize the NAO. Therefore, a

similar influence of the EAWR on storm surge, tropical cyclone frequency, and local wind stress as the NAO [33] is not unexpected but does deserve additional research.

A strong and spatially coherent link between long-term sea levels and the EAWR was also identified along the southern coast of Alaska in the northeast Pacific. Although the exact mechanism responsible for this apparent link is not immediately obvious, it is possible that, based on the findings of Ezer et al. [36] regarding a potential link between ENSO and the NAO, which results in sea level variability along the northern East Coast that coincides with the phases of ENSO, a similar link may exist between the EAWR and ENSO or the PDO, resulting in an indirect effect on northern Pacific sea levels. More research is required to verify the specific teleconnection responsible.

Due to the limited amount of data available to analyze each epoch, some caution needs to be taken when assessing the final results in terms of both correlation strength and significance. The dominant CIs that were identified during the most recent epoch are considered more trustworthy due to the fact that there is much more spatial coherence in addition to consistency with the results for the entire period of record; the results for the earlier epochs show less spatial coherence and consistency with the full analysis, and therefore, are considered less reliable.

In addition to identifying potential mechanisms of climate variability responsible for short-term changes in coastal sea levels throughout North America, it was also found using trend analysis that sea levels experienced long-term changes over the course of the study period, which is consistent with the conclusions of previous studies [9,10,38,46]. One key aspect observed from the trend analysis was the presence of stations where coastal sea levels remained stable throughout a given epoch even though they are located relatively close to stations where significant sea level rise occurred (see Figure 6). This finding does not necessarily indicate irreversible stability in coastal sea levels at the local scale. For example, the stations at Vancouver in southwestern Canada and South Beach in the southeastern US exhibited stable coastal sea level conditions during the 1971–1994 epoch, but coastal sea level rise did eventually occur during the 1995–2018 epoch. This behavior implies that these changes are likely not related to local factors, such as land subsidence due to increased development, but potentially to larger-scale phenomena such as isostatic rebound, glacial and ice sheet melt, and/or changes in ocean dynamics, though additional research is required to validate this assumption.

## 5. Conclusions

There is a lack of knowledge and data to identify communities and locations most at risk from coastal hazards related to sea level rise. Still, this knowledge is crucial to make planning decisions both now and in the future. Understanding the drivers of risk in these highly diverse coastal areas is socioeconomically essential. Due to the projected impacts of climate change on mean sea levels, it is essential to be aware of the underlying mechanisms related to climate variability that can be linked to short- and long-term fluctuations in sea levels, on top of which the potential effects of climate change can be superimposed.

In an attempt to understand some of the underlying mechanisms related to short-term and long-term sea level variability and whether they are consistent over time, potential links between several climate indices (CIs) and long-term coastal sea levels were assessed during the study period 1948–2018 as well as three consecutive epochs within this period: 1948–1970, 1971–1994, and 1995–2018. The CIs considered in the current study either characterized SSTs over portions of the Pacific and/or Atlantic Oceans as well as the Caribbean or atmospheric behavior in terms of height and pressure anomalies over the northern Pacific and Atlantic Oceans. Focusing on the entire period of record as well as the most recent epoch due to higher data availability, the Western Hemisphere Warm Pool (WHWP), which characterizes SSTs within and beyond the western and eastern boundaries of the Caribbean, exhibited a dominant link with sea levels along the entire US West and East Coasts, with particular emphasis along the East Coast south of Cape Hatteras during the final epoch. This can be attributed to a potential link with ENSO in the Pacific Ocean

and the influence of SSTs within the WHWP on the strength of the Florida Current in the Caribbean and Atlantic Ocean. North of Cape Hatteras, the Eastern Atlantic Western Russia pattern (EAWR), which is partially characterized by a region of height anomalies over the North Atlantic, exhibited a dominant signal during the final epoch even beyond what has been previously found regarding the influence of the NAO during the same time period. This is not surprising as the locations of atmospheric conditions characterized by each CI are adjacent to each other, though previous research has only focused on the NAO. What is a more unexpected is the fact that the EAWR also exhibited strong signals with sea coastal sea levels in the Northeast Pacific along the southern coast of Alaska. Some ideas with regard to potential mechanisms were proposed, but additional research is required to confirm the influence of these or other possible teleconnections.

During the epochs of 1948–1970, 1971–1994, and 1995–2018, mean coastal sea levels derived from PSMSL tide gauge stations along the coasts of North America showed differences in magnitude and sign. For the first epoch, most of these showed upward trends in the northeastern US and Canada coastal regions. Over 1971–1994 we found upward trends along the Southern California coast. Between 1995 and 2018, the eastern and western US, including Hawaii, exhibited upward trends in coastal sea levels. An opposite or stable signal was dominant in Canada's Atlantic and Pacific coastal regions.

The initial epoch observed an increase in coastal sea levels at 24 sites, while subsequent epochs recorded increases at 26 and 58 sites, respectively. The Atlantic Multidecadal Oscillation (AMO) dominated 25% of the increasing trend sites during the first epoch, with the Caribbean Oscillation (CAR) and Pacific Decadal Oscillation (PDO) each contributing to 21%. In the second epoch, the Western Hemisphere Warm Pool (WHWP) primarily influenced 19.23% of sites, the East Asian Winter Monsoon (EAWR) impacted 15.38%, and both the North Pacific Index (N12) and Northern Oscillation Index (NOI) accounted for 11.54%. In the final epoch, the WHWP predominated in 43.10% of sites, followed by the EAWR at 20.6% and the CAR at 10.34%. These findings emphasize a discernible shift in dominant CIs affecting coastal sea level trends and highlight the need for a comprehensive understanding of the driving forces. Further research is necessary to better understand the varied influences of regional climate oscillations on coastal sea levels and their potential implications for coastal communities.

The results from this study may provide useful information in potentially being able to predict long-term future trends and variability in mean sea levels throughout North America and thus should encourage and help to focus additional research regarding those CIs found to have the strongest links with sea level variability in this part of the globe.

**Supplementary Materials:** The following supporting information can be downloaded at: https://www.mdpi.com/article/10.3390/cli11040080/s1, Table S1: The table presents trend analysis results for North American coastal sites during the 1948–1970 epoch, featuring the dominant climate index (CI), linear correlation coefficient (r) between coastal sea level and CI, Theil-Sen slope estimator, confidence intervals (CI) for Theil-Sen slope, and Modified Mann-Kendall (MK) trend test p-value for each site. Country and site name are also provided. Table S2: As in Suppl. Table S1 but for the 1971–1994 epoch. Table S3: As in Suppl. Table S1 but for the 1995–2018 epoch.

**Author Contributions:** Conceptualization: J.G. and F.P.-T.; methodology: J.G. and F.P.-T.; software: J.G. and F.P.-T.; validation: J.G. and F.P.-T.; formal analysis: J.G. and F.P.-T.; investigation: F.P.-T.; data curation: F.P.-T.; writing—original draft: J.G., F.P.-T., V.E.A. and C.A.C.d.S.; writing—review & editing: J.G., F.P.-T., V.E.A. and C.A.C.d.S.; visualization: F.P.-T.; project administration: J.G.; funding acquisition: F.P.-T. All authors have read and agreed to the published version of the manuscript.

**Funding:** This research was partially funded by the Research Productivity Grant (Grant No. 304493/2019-8) provided by the Brazilian National Council for Scientific and Technological Development (CNPq).

**Institutional Review Board Statement:** Not applicable.

**Informed Consent Statement:** Not applicable.

**Data Availability Statement:** The data (climate indices and sea levels) used in this study are publicly available at [45,48], respectively.

**Acknowledgments:** The authors would like to thank the International Center for Integrated Water Resources Management (ICI-WaRM) for facilitating the development of the ICI-Warm Regional Analysis of Frequency Tool (ICI-RAFT) (https://www.iwr.usace.army.mil/Missions/Hydrology/ICI-RAFT-ICIWaRM-Regional-Analysis-of-Frequency-T/; accessed on 1 July 2014), which inspired us and was used to validate the development and accuracy of Hydro-CLIM.

**Conflicts of Interest:** The authors declare no conflict of interest.

## References

1. World Bank. *Building Resilience: Integrating Climate and Disaster Risk into Development*; World Bank: Washington, DC, USA, 2013.
2. Kelman, I.; Gaillard, J.C.; Mercer, J. Climate Change's Role in Disaster Risk Reduction's Future: Beyond Vulnerability and Resilience. *Int. J. Disaster Risk Reduct.* **2015**, *6*, 21–27. [CrossRef]
3. Reguero, B.G.; Losada, I.J.; Díaz-Simal, P.; Méndez, F.J.; Beck, M.W. Effects of Climate Change on Exposure to Coastal Flooding in Latin America and the Caribbean. *PLoS ONE* **2015**, *10*, e0133409. [CrossRef] [PubMed]
4. UNFPA (United Nations Fund for Population Activities). *Linkages between Population Dynamics, Urbanization Processes and Disaster Risks: A Regional Vision of Latin America*; UN-HABITAT, ISDR, UNFPA: New York, NY, USA, 2012.
5. Cazenave, A.; Cozannet, G.L. Sea level rise and its coastal impacts. *Earth's Future* **2014**, *2*, 15–34. [CrossRef]
6. Church, J.A.; Clark, P.U.; Cazenave, A.; Gregory, J.M.; Jevrejeva, S.; Levermann, A.; Merrifield, M.A.; Milne, G.A.; Nerem, R.S.; Nunn, P.D.; et al. Sea level change. In *Climate Change 2013: The Physical Science Basis. Contribution of Working Group I to the Fifth Assessment Report of the Intergovernmental Panel on Climate Change*; Stocker, T.F., Qin, D., Plattner, G.-K., Tignor, M., Allen, S.K., Boschung, J., Nauels, A., Xia, Y., Bex, V., Midgley, P.M., Eds.; Cambridge University Press: Cambridge, UK; New York, NY, USA, 2013; pp. 1137–1216.
7. Seneviratne, S.I.; Nicholls, N.; Easterling, D.; Goodess, C.M.; Kanae, S.; Kossin, J.; Luo, Y.; Marengo, J.; McInnes, K.; Rahimi, M.; et al. Changes in climate extremes and their impacts on the natural physical environment. In *Managing the Risks of Extreme Events and Disasters to Advance Climate Change Adaptation. A Special Report of Working Groups I and II of the Intergovernmental Panel on Climate Change (IPCC)*; Field, C.B., Barros, V., Stocker, T.F., Qin, D., Dokken, D.J., Ebi, K.L., Mastrandrea, M.D., Mach, K.J., Plattner, G.-K., Allen, S.K., Tignor, M., Midgley, P.M., Eds.; Cambridge University Press: Cambridge, UK; New York, NY, USA, 2012; pp. 109–230.
8. Merkens, J.-L.; Reimann, L.; Hinkel, J.; Vafeidis, A.T. Gridded population projections for the coastal zone under the Shared Socioeconomic Pathways. *Glob. Planet. Chang.* **2016**, *145*, 57–66. [CrossRef]
9. Sallenger, A.H.; Doran, K.S.; Howd, P.A. Hotspot of accelerated sea-level rise on the Atlantic coast of North America. *Nat. Clim. Chang.* **2012**, *2*, 884–888. [CrossRef]
10. Becker, M.; Karpytchev, M.; Papa, F. Hotspots of relative sea level rise in the tropics. In *Tropical Extremes: Natural Variability and Trends*; Venugopal, V., Sukhatme, J., Murtugudde, R., Roca, R., Eds.; Elsevier: Amsterdam, The Netherlands, 2019; pp. 203–262.
11. Kirezci, E.; Young, I.R.; Ranasinghe, R.; Muis, S.; Nicholls, R.J.; Lincke, D.; Hinkel, J. Projections of global-scale extreme sea levels and resulting episodic coastal flooding over the 21st Century. *Sci. Rep.* **2020**, *10*, 11629. [CrossRef] [PubMed]
12. Hauer, M.E.; Evans, J.M.; Mishra, D.R. Millions projected to be at risk from sea-level rise in the continental United States. *Nat. Clim. Chang.* **2016**, *6*, 691–695. [CrossRef]
13. Nagy, G.J.; Gutiérrez, O.; Brugnoli, E.; Verocai, J.E.; Gómez-Erache, M.; Villamizar, A.; Olivares, I.; Azeiteiro, U.M.; Filho, W.L.; Amaro, N. Climate vulnerability, impacts and adaptation in Central and South America coastal áreas. *Reg. Stud. Mar. Sci.* **2019**, *29*, 100683. [CrossRef]
14. Wong, P.P.; Losada, I.J.; Gattuso, J.-P.; Hinkel, J.; Khattabi, A.; McInnes, K.L.; Saito, Y.; Sallenger, A. Coastal systems and low-lying areas. In *Climate Change 2014: Impacts, Adaptation and Vulnerability. Part A: Global and Sectoral Aspects. Working Group II. Contribution to the Fifth Assessment Report of the Intergovernmental Panel on Climate Change*; Field, C.B., Barros, V.R., Dokken, D.J., Mach, K.J., Mastrandrea, M.D., Bilir, T.E., Chatterjee, M., Ebi, K.L., Estrada, Y.O., Genova, R.C., et al., Eds.; Cambridge University Press: Cambridge, UK, 2014; pp. 361–409.
15. Watson, P.J. Acceleration in US mean sea level? A new insight using improved tools. *J. Coast. Res.* **2016**, *32*, 1247–1261. [CrossRef]
16. Oppenheimer, M.; Glavovic, B.C.; Hinkel, J.; van de Wal, R.; Magnan, A.K.; Abd-Elgawad, A.; Cai, R.; Cifuentes-Jara, M.; DeConto, R.M.; Ghosh, T.; et al. Sea Level Rise and Implications for Low-Lying Islands, Coasts and Communities. In *IPCC Special Report on the Ocean and Cryosphere in a Changing Climate*; Pörtner, H.-O., Roberts, D.C., Masson-Delmotte, V., Zhai, P., Tignor, M., Poloczanska, E., Mintenbeck, K., Alegría, A., Nicolai, M., Okem, A., et al., Eds.; Cambridge University Press: Cambridge, UK; New York, NY, USA, 2019; pp. 321–445.
17. Wallace, J.M.; Rasmusson, E.M.; Mitchell, T.P.; Kousky, V.E.; Sarachik, E.S.; von Storch, H.J. On the structure and evolution of ENSO-related climate variability in the tropical Pacific: Lessons from TOGA. *Geophys. Res.* **1998**, *103*, 14241–14259. [CrossRef]
18. Merrifield, M.A.; Thompson, P.R. Interdecadal sea level variations in the Pacific: Distinctions between the tropics and extratropics. *Geophys. Res. Lett.* **2018**, *45*, 6604–6610. [CrossRef]

19. Sweet, W.W.V.; Dusek, G.; Obeysekera, J.T.B.; Marra, J.J. *NOAA Technical Report NOS CO-OPS 086: Patterns and Projections of High Tide Flooding along the US Coastline Using a Common Impact Threshold*; National Oceanographic and Atmospheric Administration: Silver Spring, MD, USA, 2018.
20. Khouakhi, A.; Villarini, G.; Zhang, W.; Slater, L.J. Seasonal predictability of high sea level frequency using ENSO patterns along the US West Coast. *Adv. Water Resour.* **2019**, *131*, 103377. [CrossRef]
21. Bromirski, P.D.; Miller, A.J.; Flick, R.E.; Auad, G. Dynamical suppression of sea level rise along the Pacific coast of North America: Indications for imminent acceleration. *J. Geophys. Res. Ocean.* **2011**, *116*, C07005. [CrossRef]
22. Moon, J.-H.; Song, Y.T.; Lee, H. PDO and ENSO modulations intensified decadal sea level variability in the tropical Pacific. *J. Geophys. Res. Ocean.* **2015**, *120*, 8229–8237. [CrossRef]
23. Buckley, M.W.; Marshall, J. Observations, inferences, and mechanisms of Atlantic Meridional Overturning Circulation variability: A review. *Rev. Geophys.* **2016**, *54*, 5–63. [CrossRef]
24. NOAA (National Oceanographic and Atmospheric Administration): Climate Indices: Monthly Atmospheric and Ocean Time Series. Available online: https://psl.noaa.gov/data/climateindices/list/ (accessed on 16 February 2016).
25. Little, C.M.; Hu, A.; Hughes, C.W.; McCarthy, G.D.; Piecuch, C.G.; Ponte, R.M.; Thomas, M.D. The Relationship Between U.S. East Coast Sea Level and the Atlantic Meridional Overturning Circulation: A Review. *Geophys. Res. Lett.* **2019**, *124*, 6435–6458. [CrossRef] [PubMed]
26. Smith, K.L.; Polvani, L.M. Modeling evidence for large, ENSO-driven interannual wintertime AMOC variability. *Environ. Res. Lett.* **2021**, *16*, 084038. [CrossRef]
27. Hamlington, B.D.; Leben, R.R.; Kim, K.Y.; Nerem, R.S.; Atkinson, L.P.; Thompson, P.R. The effect of the El Nino-Southern Oscillation on US regional and coastal sea level. *J. Geophys. Res. Ocean.* **2015**, *120*, 3970–3986. [CrossRef]
28. Kennedy, A.J.; Griffin, M.L.; Morey, S.L.; Smith, S.R.; O'Brien, J.J. Effects of El Niño–Southern Oscillation on sea level anomalies along the Gulf of Mexico coast. *J. Geophys. Res. Ocean.* **2007**, *112*, C05047. [CrossRef]
29. Menéndez, M.; Woodworth, P.L. Changes in extreme high water levels based on a quasi-global tidegauge data set. *J. Geophys. Res. Ocean.* **2010**, *115*, C10011. [CrossRef]
30. Muis, S.; Haigh, I.D.; Nobre, G.G.; Aerts, J.C.J.H.; Ward, P.J. Influence of El Niño–Southern Oscillation on global coastal flooding. *Earths Future* **2018**, *6*, 1311–1322. [CrossRef]
31. Sweet, W.; Park, J. From the extreme to the mean: Acceleration and tipping points of coastal inundation from sea level rise. *Earths Future* **2014**, *2*, 579–600. [CrossRef]
32. Hurrell, J.W. Decadal Trends in the North Atlantic Oscillation: Regional Temperatures and Precipitation. *Science* **1995**, *269*, 676–679. [CrossRef] [PubMed]
33. Pinto, J.G.; Zacharias, S.; Fink, A.H.; Leckebusch, G.C.; Ulbrich, U. Factors contributing to the development of extreme North Atlantic cyclones and their relationship with the NAO. *Clim. Dyn.* **2009**, *32*, 711–737. [CrossRef]
34. Kenigson, J.S.; Han, W.; Rajagopalan, B.; Yanto, M.; Jasinski, M. Decadal Shift of NAO-Linked Interannual Sea Level Variability along the US Northeast Coast. *J. Clim.* **2018**, *31*, 4981–4989. [CrossRef]
35. Sweet, W.V.; Horton, R.; Kopp, R.E.; LeGrande, A.N.; Romanou, A. Sea level rise. In *Climate Science Special Report: Fourth National Climate Assessment*; Wuebbles, D.J., Fahey, D.W., Hibbard, K.A., Dokken, D.J., Stewart, B.C., Maycock, T.K., Eds.; USGCRP: Washington, DC, USA, 2017; Volume 1, pp. 333–363.
36. Ezer, T.; Atkinson, L.P.; Corlett, W.B.; Blanco, J.L. Gulf Stream's induced sea level rise and variability along the US mid-Atlantic coast. *J. Geophys. Res. Ocean.* **2013**, *118*, 685–697. [CrossRef]
37. Wang, C.; Enfield, D.B. The Tropical Western Hemisphere Warm Pool. *Geophys. Res. Lett.* **2001**, *28*, 1635–1638. [CrossRef]
38. Domingues, R.; Goni, G.; Baringer, M.; Volkov, D. What Caused the Accelerated Sea Level Changes Along the U.S. East Coast During 2010–2015? *Geophys. Res. Lett.* **2018**, *45*, 13367–13376. [CrossRef]
39. Enfield, D.B.; Lee, S.K.; Wang, C. How are large western hemisphere warm pools formed? *Prog. Oceanogr.* **2006**, *70*, 346–365. [CrossRef]
40. Volkov, D.L.; Baringer, M.; Smeed, D.; Johns, W.; Landerer, F.W. Teleconnection between the Atlantic Meridional Overturning Circulation and sea level in the Mediterranean Sea. *J. Clim.* **2019**, *32*, 935–955. [CrossRef]
41. Fenoglio-Marc, L.; Tel, E. Coastal and global sea level change. *J. Geodyn.* **2010**, *49*, 151–160. [CrossRef]
42. Wilcox, R. A note on the Theil-Sen regression estimator when the regressor is random and the error term is heteroscedastic. *Biom. J.* **1998**, *40*, 261–268. [CrossRef]
43. Hünicke, B.; Zorita, E. Trends in the amplitude of Baltic Sea level annual cycle. *Tellus A Dyn. Meteorol. Oceanogr.* **2008**, *60*, 154–164. [CrossRef]
44. Yue, S.; Wang, C. The Mann-Kendall test modified by effective sample size to detect trend in serially correlated hydrological series. *Water Resour. Manag.* **2004**, *18*, 201–218. [CrossRef]
45. Hamed, K.H.; Rao, A.R. A modified Mann-Kendall trend test for autocorrelated data. *J. Hydrol.* **1998**, *204*, 182–196. [CrossRef]
46. Joshi, N.; Kalra, A.; Thakur, B.; Lamb, K.W.; Bhandari, S. Analyzing the Effects of Short-Term Persistence and Shift in Sea Level Records along the US Coast. *Hydrology* **2021**, *8*, 17. [CrossRef]
47. Aksoy, A.O. Investigation of sea level trends and the effect of the north Atlantic oscillation (NAO) on the black sea and the eastern Mediterranean Sea. *Theor. Appl. Climatol.* **2017**, *129*, 129–137. [CrossRef]

48. Taibi, H.; Haddad, M. Estimating trends of the Mediterranean Sea level changes from tide gauge and satellite altimetry data (1993–2015). *JOL* **2019**, *37*, 1176–1185. [CrossRef]
49. Lobeto, H.; Menéndez, M.; Losada, I.J. Toward a methodology for estimating coastal extreme sea levels from satellite altimetry. *J. Geophys. Res. Ocean.* **2018**, *123*, 8284–8298. [CrossRef]
50. PSMSL (Permanent Service for Mean Sea Level): Tide Gauge Data. Available online: https://www.psmsl.org/data/ (accessed on 1 May 2020).
51. Holgate, S.J.; Matthews, A.; Woodworth, P.L.; Rickards, L.J.; Tamisiea, M.E.; Bradshaw, E.; Foden, P.R.; Gordon, K.M.; Jevrejeva, S.; Pugh, J. New Data Systems and Products at the Permanent Service for Mean Sea Level. *J. Coast. Res.* **2012**, *29*, 493.
52. IPCC. *Climate Change 2021: The Physical Science Basis. Contribution of Working Group I to the Sixth Assessment Report of the Intergovernmental Panel on Climate Change*; Masson-Delmotte, V., Zhai, P., Pirani, A., Connors, S.L., Péan, C., Berger, S., Caud, N., Chen, Y., Goldfarb, L., Gomis, M.I., et al., Eds.; Cambridge University Press: Cambridge, UK; New York, NY, USA, 2021.
53. Giovannettone, J.P.; Zhang, Y. Identifying strong signals between low-frequency climate oscillations and annual precipitation using long-window correlation analysis. *Int. J. Climatol.* **2019**, *39*, 4883–4894. [CrossRef]
54. Giovannettone, J.P.; Paredes-Trejo, F.; Barbosa, H.; dos Santos, C.A.C.; Kumar, T.V.L. Characterization of links between hydro-climate indices and long-term precipitation in Brazil using correlation analysis. *Int. J. Climatol.* **2020**, *40*, 5527–5541. [CrossRef]
55. Giovannettone, J.P. Assessing the relationship between low-frequency oscillations of global hydro-climate indices and long-term precipitation throughout the United States. *JAMC* **2021**, *60*, 87–101.
56. Efron, B. Estimating the error rate of a prediction rule: Improvement on cross-validation. *JASA* **1983**, *78*, 316–331. [CrossRef]
57. Efron, B. Bootstrap methods: Another look at the jackknife. *Ann. Stat.* **1979**, *7*, 569–593. [CrossRef]
58. Enfield, D.B.; Mestas-Nuñez, A.M.; Trimble, P.J. The Atlantic multidecadal oscillation and its relation to rainfall and river flows in the continental U.S. *Geophys. Res. Lett.* **2001**, *28*, 2077–2080. [CrossRef]
59. Giovannettone, J.P. *HydroMetriks—Climate Tool (Hydro-CLIM)*; HydroMetriks, LLC.: Silver Spring, MD, USA, 2020.
60. Chambers, D.P.; Merrifield, M.A.; Nerem, R.S. Is there a 60-year oscillation in global mean sea level? *Geophys. Res. Lett.* **2012**, *39*, L18607. [CrossRef]
61. Pan, H.; Lv, X. Is there a quasi 60-year oscillation in global tides? *Cont. Shelf Res.* **2021**, *222*, 104433. [CrossRef]
62. Park, J.-H.; Kug, J.-S.; Li, T.; Behera, S.K. Predicting El Niño Beyond 1-year Lead: Effect of the Western Hemisphere Warm Pool. *Sci. Rep.* **2018**, *8*, 14957. [CrossRef]
63. Cleveland, W.S. 1981 LOWESS: A program for smoothing scatter plots by robust locally weighted regression. *Am. Stat.* **1981**, *35*, 54. [CrossRef]
64. Park, J.-H.; Kug, J.-S.; An, S.I.; Li, T. Role of the western hemisphere warm pool in climate variability over the western North Pacific. *Clim. Dyn.* **2019**, *53*, 2743–2755. [CrossRef]